Title

Extracellular matrix downregulation in the Drosophila heart preserves contractile function and improves lifespan

Authors

Sessions, Ayla O
Kaushik, Gaurav
Parker, Sarah
et al.

Publication Date

2017

DOI

10.1016/j.matbio.2016.10.008

Peer reviewed

Extracellular matrix downregulation in the *Drosophila* heart preserves contractile function and improves lifespan

Ayla O. Sessions[a], Gaurav Kaushik[b], Sarah Parker[c], Koen Raedschelders[c], Rolf Bodmer[d], Jennifer E. Van Eyk[c] and Adam J. Engler[a,b,e]

a - Biomedical Sciences Program, *UC, San Diego; La Jolla, CA 92093, USA*
b - Department of Bioengineering, *UC, San Diego; La Jolla, CA 92093, USA*
c - Advanced Clinical Biosystems Research Institute; Barbra Streisand Women's Heart Center; Cedars-Sinai Heart Institute; Cedars-Sinai Medical Center; Los Angeles, *CA 90048, USA*
d - Development, *Aging, and Regeneration Program, Sanford Burnham Prebys Medical Discovery Institute; La Jolla, CA 92037, USA*
e - Sanford Consortium for Regenerative Medicine, *La Jolla, CA 92037, USA*

Correspondence to Adam J. Engler: *at: Biomedical Sciences Program, UC, San Diego; La Jolla, CA 92093, USA.*
aengler@ucsd.edu
http://dx.doi.org/10.1016/j.matbio.2016.10.008

Abstract

Aging is associated with extensive remodeling of the heart, including basement membrane (BM) components that surround cardiomyocytes. Remodeling is thought to impair cardiac mechanotransduction, but the contribution of specific BM components to age-related lateral communication between cardiomyocytes is unclear. Using a genetically tractable, rapidly aging model with sufficient cardiac genetic homology and morphology, e.g. *Drosophila melanogaster*, we observed differential regulation of BM collagens between laboratory strains, correlating with changes in muscle physiology leading to cardiac dysfunction. Therefore, we sought to understand the extent to which BM proteins modulate contractile function during aging. Cardiac-restricted knockdown of ECM genes *Pericardin*, *Laminin A*, and *Viking* in *Drosophila* prevented age-associated heart tube restriction and increased contractility, even under viscous load. Most notably, reduction of *Laminin A* expression correlated with an overall preservation of contractile velocity with age and extension of organismal lifespan. Global heterozygous knockdown confirmed these data, which provides new evidence of a direct link between BM homeostasis, contractility, and maintenance of lifespan.

Introduction

Aging is associated with the progressive decline of cardiac performance [1]. Reduced cardiac output is observed in species ranging from complex vertebrates down to simple invertebrates because of conserved cellular and molecular alterations [2,3]. Aging has also been associated with aberrant interstitial extracellular matrix (ECM) expression and assembly, leading to stiffer, less contractile muscle [4,5]. The basement membrane (BM) is a thin layer of ECM that surrounds the lateral surfaces of cardiomyocytes; while mutations in BM components, e.g. Collagen IV, result in cardiovascular disease [6,7], the role of specific components has remained largely unstudied, especially during aging. From what is known, Collagen IV expression increases with age in mice and is correlated with a thickening of cardiac BM [8]. Humans of advanced age in heart failure also experience an increase in Laminin and Collagen IV protein content within the heart relative to their age-matched counterparts [9]. Taken together these data suggest that cardiac BM remodeling in response to pressure and load could be conserved with age. Conserved ECM alterations may compensate for age-associated damage similar to cytoskeletal proteins, e.g. Vinculin [10], but it is not yet clear whether certain BM protein changes are beneficial or deleterious to cardiac function with physiological aging. So to build consensus on ECM-based mechanisms of

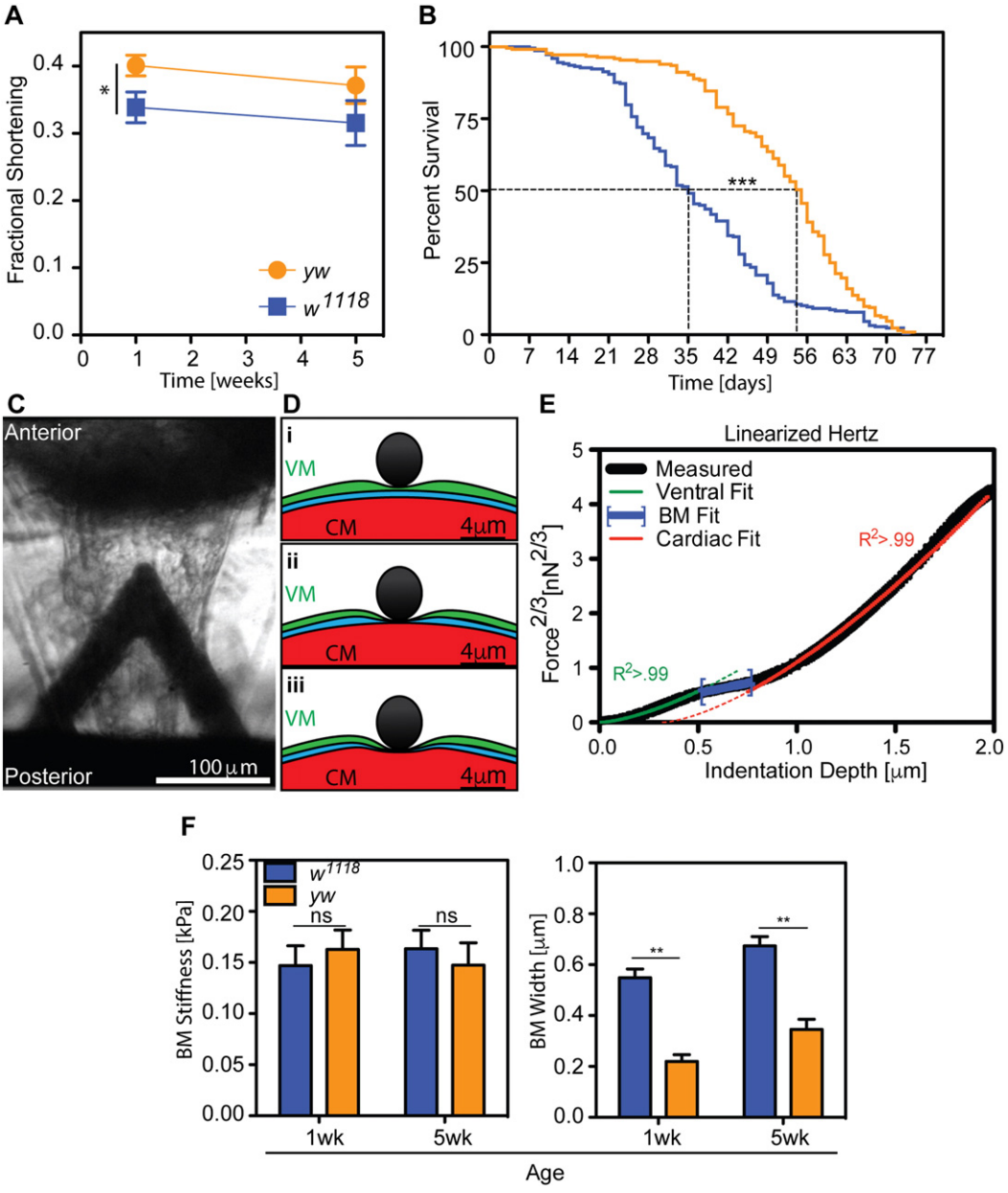

Fig. 1. Decreased fractional shortening in w^{1118} correlates with decreased longevity and increased BM thickness. (A) Fractional shortening was calculated for each genotype and age (mean ± s.e.m., n = 20) and is plotted at 1 and 5 weeks. * $p < 0.05$ (B) Survival curves for indicated wildtypes show median survival indicated by the dashed black line for each genotype, 55 and 35 days for *yw* (n = 215) and w^{1118} (n = 223), respectively. ***$p < 0.001$. (C) Brightfield image of AFM cantilever (open triangular shape) positioned over midline (center) of the *Drosophila* heart tube during nanoindentation analysis of *Drosophila* tri-layered myocardium. Scale bar is 100 µm. (D) Schematic of 3 layered AFM nanoindentation (black circle) into *Drosophila* heart tube depicting: (i) the 1st layer indentation of the VM, (ii) the complete compaction of the VM layer and 2nd layer indentation of the BM, and (iii) the final compaction of the first 2 layers and 3rd layer indentation of the CM layer. (E) A representative force vs. indentation depth plot in black showing the respective Linearized-Hertz fits for both the shallow (green) VM and deep (red) CM with a BM layer indicated by a linear region shown in blue starting and ending within the brackets. (F) BM stiffness and BM thickness reported as the length over which the BM linear region was fit were measured by AFM at the ventral midline and plotted at indicated ages. All data represented as mean ± s.e.m. of >15 flies.*$p < 0.05$ and **$p < 0.01$ for indicated comparisons.

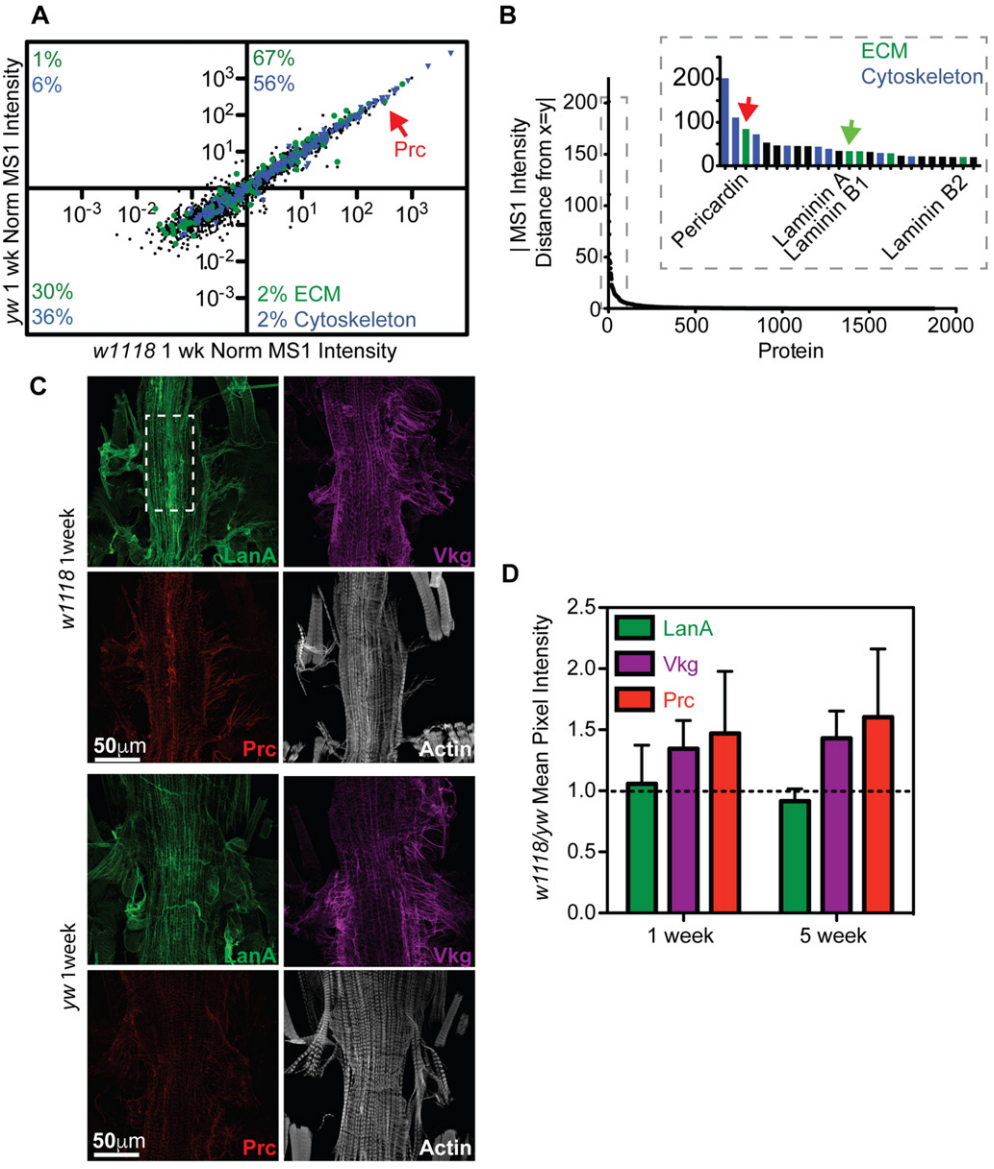

Fig. 2. Cardiac basement membrane protein regulation differences in wildtype *Drosophila*. (A) Scatter plot of the MS1 intensity values for each protein. MS1 intensity values (protein abundance) are plotted for w^{1118} value on the x-axis and *yw* value on the y-axis. Colors of points indicate biological function as determined by Software Tool for Rapid Annotation of Proteins (STRAP) analysis and relative percentages in each quadrant are given (ECM - green, Cytoskeleton - blue). Red arrow indicates Pericardin [Prc]. Data represents a mean value of 4 biological replicates of 50 pooled fly hearts for protein analysis. (B) Absolute distance of MS1 intensity values from a zero $\log_2$ fold change or x = y were plotted for each protein in decreasing fashion. 25 proteins with highest calculated distance values are shown in subpanel (gray dashed box) color coded by STRAP analysis (ECM - green, Cytoskeleton - blue) with ECM proteins of interest listed on the x-axis and Laminin A (the cardiac specific laminin subunit within trimer) highlighted with green arrow and Pericardin in red arrow. (C) Representative immunofluorescent images for the indicated genotypes at 1 week for proteins Laminin A (green), Viking (purple), Pericardin (red), and F-actin (white). All fluorescent intensities were normalized to F-actin within region of interest (ROI) selected over bulk of heart tube (top left, white dashed box). Scale bar is 50 μm. (D) Mean pixel intensity for each indicated protein as measured within ROI, normalized to F-actin intensity within ROI, and shown as w^{1118} normalized to *yw*. Mean F-actin intensity varied <10% sample to sample between each genotype or with age. n = 4 hearts per comparison.

age-associated but non-pathological remodeling, we used a rapidly aging system where cardiac BM proteins could be controllably expressed and myocyte function assessed in situ.

Model organisms like *Drosophila melanogaster* can be extremely useful to understand the cell biology of cardiac aging given their genetic tractability, rapid aging, and conserved cardiac proteome, which has >80% protein domain homology with mice [11]. Its heart consists of bilateral rows of contractile cardiomyocytes (CM) that form a 40–120 μm wide linear tube in the fly abdomen (Supplemental Fig. S1, A and B). Though the heart tube morphology differs from mammals, its simplicity allows for rapid measurement of cardiac parameters [12] and permits in situ mechanical measurement [10,13,14]. CMs are anchored to the cuticle by a non-contractile, skeletal muscle-derived, and longitudinally-oriented layer of 10–12 ventral muscle fibers (VM; Supplemental Fig. S1, B-D) [14–16]. Separating these muscle layers is a densely packed, thin BM that adheres the lateral surfaces of CMs to the VM and surrounds the VM fibers (Supplemental Fig. S1, B and D) [16]. Manipulation of BM proteins can result in partial to complete loss of heart tube structure. For example, global loss of the cardiac specific subunit of the laminin trimer, *Laminin A*, prevents tube formation [17,18]. Additionally, global mutations or knockdown in either of two Collagen IV genes, *Cg25C* or *Viking*, weaken cardiac ECM assembly [19] by perturbing Perlecan, a BM proteoglycan, assembly [20]. In addition to typical BM components, the fly heart tube also has an outer "fibrillar-like" matrix largely composed of Pericardin, which is has domains homologous to mammalian Collagen IV [21,22]. Pericardin is also essential for tube formation [22,23] and colocalizes with other BM components on the outer BM surfaces of the heart tube. While BM and integrin expression help polarize cells during development [17,24], their function in adult *Drosophila* may be to mechanically couple CMs and VM.

Despite our limited knowledge of ECM regulation of adult *Drosophila* heart tube morphology and function, the heart tube's advantages as an aging system suggests that we can use it to rapidly screen BM-dependent cardiac aging phenotypes relevant to mammals. The reduced number of collagen and laminin genes versus higher organisms also simplifies genetic perturbations and can ensure cardiac specificity. Thus, we sought to characterize BM in the adult *Drosophila* heart and hypothesized that BM components directly affect age-related myocyte extracellular interactions and cardiac function. As with advanced aged humans with heart disease, we found that some BM proteins are increased in the adult hearts for some wild-type *Drosophila melanogaster* strains (i.e. w^{1118} versus *yw* strains), as with *macaca mulatta* and to a lesser extent with *rattus norvegicus*, and this correlated with increased BM thickness and decreased contraction. Restricting cardiac expression of *Pericardin*, *Laminin A*, and *Viking* in w^{1118} flies resulted in thinner BM, increased contractile capacity with age, and significantly increased lifespan, which suggests a closer relationship between BM expression and CM function.

Results

Genotype-dependent BM expression correlates with altered muscle morphology, impaired contractility, and decreased lifespan

Age-related differences in heart function occur between the common *Drosophila* wildtype lab strains *yw* and w^{1118} [10,14] and include decreased fractional shortening and significantly shortened lifespan for w^{1118} flies (Fig. 1, A and B). By adapting our biphasic analysis method for atomic force microscopy (AFM) [13,14] to fit three layers, we were able to determine the mechanics of the BM between muscle layers (Fig. 1C-E). We found that the BM layer between VM and CMs layers was thicker in w^{1118} flies–determined by the change in probe indentation depth–but independent of age. However, BM layer stiffness was unaffected by genotype or age and remained relatively soft (Fig. 1F).

Due to correlations between BM thickness, cardiac compliance, and lifespan, we then characterized proteomic changes that could drive genotype-specific cardiac BM differences. Cardiac protein expression patterns were assessed by orbitrap mass spectrometry (MS) to quantify protein accumulation differences that may not be reflected in genetic analyses; only 1-week-old adults were analyzed since BM phenotype seemed age-independent for w^{1118}. 1872 nonredundant proteins were quantified (Supplemental Tables S1 and S2) via MS for each genotype. We used STRAP (Software Tool for Rapid Annotation of Proteins) analysis [25] to identify the most enriched ontologies on a median normalized scatter plot of MS1 intensities. Cytoskeleton and ECM ontologies were among the most abundant proteins regardless of genotype, i.e. 67% of ECM and 56% of cytoskeletal proteins were found in the first quadrant (Fig. 2A; Supplemental Table S3) [26]. We calculated the differential expression of proteins between genotypes as the absolute distance of MS1 intensity values from identical expression, i.e. x = y (Supplemental Table S3). Pericardin and 3 distinct Laminin subunits (Laminin A, Laminin B1, and Laminin B2) were among the most differentially expressed proteins (Fig. 2B). In addition to candidate proteins, we explored other BM components based on an unbiased screen via immunoflourescent staining. We quantified protein abundance via calculation of

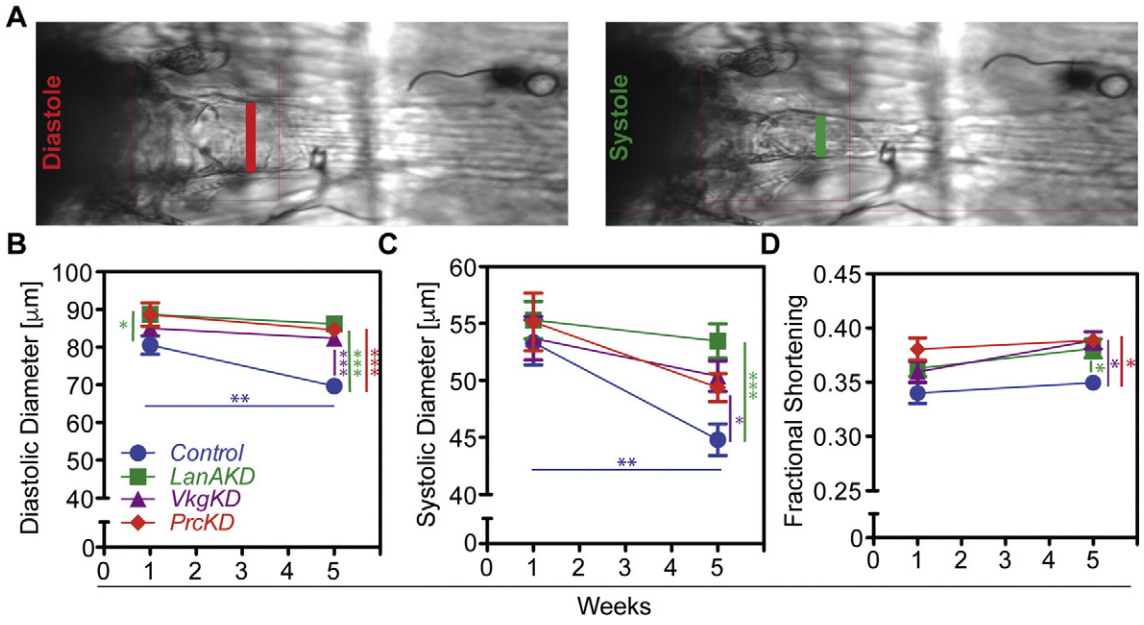

Fig. 3. High speed image analysis reveals dilated heart tube in ECM KD flies and prevention of age-related tube restriction. (A) Still ventral images of fly heart from 120 fps video capture used to create motion-mode kymographs. Lines depict where measurements for dimensions (diastole, red, and systole, green) are taken in segment a2. (B) Diastolic heart diameters were quantified at 1 and 5 weeks for indicated genotypes. (C) Systolic heart diameters were quantified at 1 and 5 weeks for indicated genotypes. (D) Fractional Shortening were quantified for indicated genotypes and ages. All data represented as mean ± s.e.m. $n > 20$. All data were analyzed via 2-way-ANOVA with post hoc Bonferroni test. Non-parametric student's two-tailed t-test was used to assess significance within each genotype with age. *$p < 0.05$, **$p < 0.01$, ***$p < 0.001$.

mean pixel intensity for each protein normalized to F-actin within a region of interest selected over the heart tube. These data confirmed that Pericardin and to a lesser extent Viking were more robustly expressed in w^{1118} flies at 1 and 5 weeks relative to their *yw* counterparts (Fig. 2, C and D, and Supplemental Fig. S2). Laminin A (the cardiac specific subunit of the laminin trimer) did not exhibit any conclusive differences between genotypes or with age as measured by average flourescent intensity. These data suggest that increased accumulation of some BM proteins could be responsible for BM thickening in w^{1118}.

ECM Knockdown decreases BM thickness, preserves contractile function with age, and extends lifespan

The role of BM collagen and laminin in modulating cardiac function with age has not been well documented. In aged, non-diseased rhesus macaque and to a lesser extent in rat myocardium, ECM proteins including BM laminin subunits and collagen chains were upregulated (Supplemental Table S4) [10]. These genes exhibit significant homology across mammalian models verified by BLAST (Supplemental Tables S5–7) [27] and provide BM structure and stability [6,17–19,28]. Given their conservation across animal models and the up-regulation of some in w^{1118} ECM, we determined what affect modulating cardiac BM production might have on function in a fly with thick cardiac BM, i.e. w^{1118}. Because homozygous mutations in either *Laminin A* or *Viking* result in embryonic lethality [18], RNA interference was instead performed for *Pericardin*, *LamininA*, and *Viking* and knockdown (KD) restricted to the fly heart using a Hand-*Gal4* driver [29,30] and the UAS expression system (Supplemental Fig. S3A). Hand-*Gal4* flies were crossed into a blank w^{1118} background as a control. 30–40% cardiac specific KD was verified by qPCR for each strain (*LanAKD*, *VkgKD*, and *PrcKD*), although *LanAKD*, which affects the entire laminin trimer, also resulted in decreased BM expression overall (Supplemental Fig. S3B). Fluorescent intensity of each BM protein from immunofluorescence decreased by 30–47% compared to controls when normalized first to F-actin, indicating fidelity between qPCR and protein assays (Supplemental Fig. S3C).

ECM expression and organization can influence organ size and function [20,31,32], so changes to cardiac tube physiology as a function of RNA interference were determined by diastolic and systolic diameter measurements (Fig. 3A) [33]. Hand-w^{1118} control flies exhibited a significant

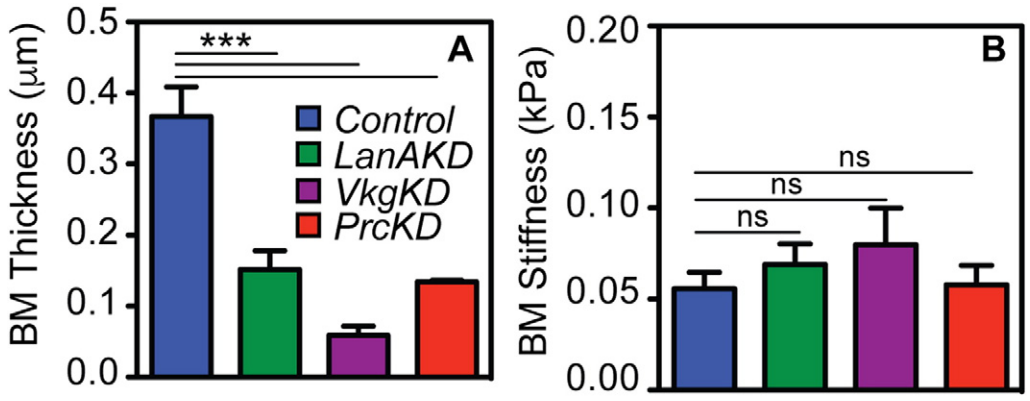

Fig. 4. Knockdown of ECM genes decreases BM thickness. (A) BM thickness reported at midline by AFM for indicated genotypes at 1 week. All KD flies were not statistically different from each other, but ***$p < 0.001$ for comparisons between KD flies and their control. (B) BM stiffness reported in kiloPascals by AFM for indicated genotypes at 1 week. All data reported as mean ± s.e.m. of >15 flies. All data analyzed with non-parametric Student's two-tailed t-test with unequal variances assumption.

reduction in diastolic and systolic dimensions with age [10,34,35] whereas *PrcKD*, *LanAKD*, or *VkgKD* flies did not (Fig. 3, B and C). Combined with a basal increase in fly heart dimensions, *PrcKD*, *LanAKD*, and *VkgKD* flies exhibited improved fractional shortening with age while control flies did not (Fig. 3D). Cardiac specific RNAi phenotypes were confirmed with using w^{1118} lines with global heterozygous deletion of genomic regions encompassing one allele for each gene, i.e. *LanA* +/−, *Vkg* +/−, and *Prc* +/− [36]. These lines have well documented down-regulation of the corresponding ECM protein [37,38]. We found up to a 70% decrease in the corresponding ECM protein when normalized to F-actin via immunofluorescent imaging in these heterozygous lines compared to w^{1118} controls (Supplemental Fig. S4A). Despite overlap with other genes in the deficient region, we observed that *LanA* +/− line had increased diastolic diameters (Supplemental Fig. S4B) and all heterozygous lines had increased fractional shortening (Supplemental Fig. S4C). Thus regardless of how BM expression is perturbed, we found that it regulates cardiac function with a similar hierarchy of phenotype changes.

The goal of RNAi mediated reduction in BM expression was to reduce BM thickness in w^{1118}. Using the tri-layered AFM analysis method, BM thickness and stiffness was measured; all KD flies experienced significant reduction BM thickness compared to control (Fig. 4A) while all remained exceedingly soft (Fig. 4B). To measure the contractile capacity for both KD and heterozygous flies, we observed hearts beating against a viscous load in situ [12]. High-speed movies from sequentially loaded hearts were converted into m-modes (Fig. 5A) so that shortening and lengthening velocities could be assessed. While genotype differences were absent for shortening velocity as a function of load at 1 week, *LanAKD* exhibited increased lengthening velocities compared to other genotypes at all loads at 1 week and demonstrated the most significant preservation in force production at all loads compared to Hand-w^{1118} controls at 5 weeks (Fig. 5B and Supplemental Table S8). Shortening velocities were also improved in *LanA*+/− flies at 1 week without viscous load (Supplemental Fig. S4D), while all heterozygous flies experienced significant increase in lengthening velocities at 1 week compared to controls (Supplemental Fig. S4E). Similarly, KD flies exhibited increased fractional shortening compared to controls (Fig. 5C). Attenuation of other matrix-related pathways and presence of transgenic drivers has correlated with organismal lifespan extension [34,39], and similarly we found that all maximum lifespans exceeded Hand-w^{1118} controls with *LanAKD* flies living the longest at 39% longer (Supplemental Table S9, Fig. 5D).

Discussion

Increased ECM deposition has been noted in heart disease [40] and aged myocardium [41], but these changes focus on fibrillar collagens and not BM proteins. We identified increased BM protein expression in non-diseased, aged rhesus macaque and rat myocardium [10], but since clarifying cardiac specific BM effects in human or mammalian models is less practical, we employed a rapidly aging model with simple cardiac physiology, i.e. *Drosophila melanogaster*. Fruit flies are well suited for a multitude of in situ mechanistic analyses not easily adapted to more complex mammalian models [10,12–14,42,43] where age [10] or ECM preference [44] may impair accurate assessment. Moreover, flies can be exceedingly sensitive; here we have demonstrated that through direct measurement of transgenic flies where *Laminin A*, *Viking*, or *Pericardin* expression was moderately reduced we

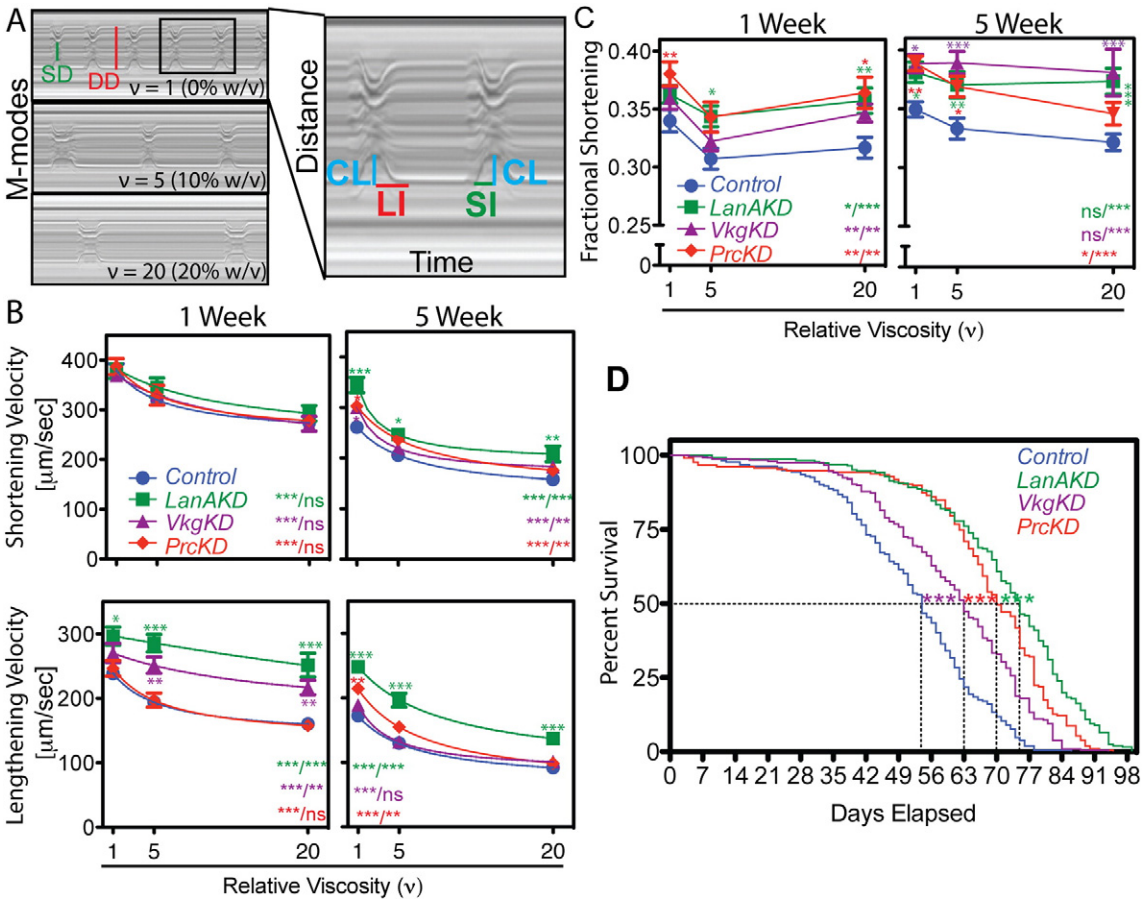

Fig. 5. ECM KD leads to preserved cardiac mechanics with age. (A) To the left, motion-mode images of a heart sequentially loaded by increasing relative viscosity, υ, by increasing Ficoll *w/v*% in the hemolymph in which the fly hearts are bathed. Arrows indicate where systole and diastole are located in the motion-mode images. To the right, m-mode image expanded to show contraction length (CL) in blue, shortening interval (SI) in green, and lengthening interval (LI) in red used for velocity measurements below. (B) Heart wall shortening (contraction) and lengthening (relaxation) velocities were assessed under viscous load and fit by Hill's model for each genotype and age. (C) Fractional shortening were measured under viscous load for each indicated genotype and age. Data represented as mean ± s.e.m. $n > 20$. All viscous load data were analyzed with 2-way-ANOVA with post hoc Bonferroni test. Significance indicates load/genotype as source of variance. *$p < 0.05$, **$p < 0.01$, ***$p < 0.001$ (D) Survival curves for indicated genotypes show median survival indicated by the dashed black line for each genotype. ***$p < 0.0001$.

observed obvious improvements in age-related heart function. Similar sensitively is found throughout the fly heart; as β1-integrin signaling is reduced via heterozygous mutations to *ILK* or *Mys* (β1-integrin), cardiac tissue stiffening attenuates and lifespan is extended [34]. Conversely when cell-ECM signaling is excessive, it can alter myocyte coupling and stiffness, leading to functional deficits [45]. Yet it is important to note that stiffness itself is not a direct indicator of dysfunction regardless of sensitivity as cytoskeleton-mediated stiffening is associated with improved function [10,31]. Despite this challenge, our data suggest that fly is a system that can precisely and accurately monitor the effects of ECM changes with age.

BM thickening is associated with impaired cardiac function

Phenotypes can vary significantly with genetic diversity, especially within laboratory-controlled lines. We found that two wildtype *Drosophila* strains–w^{1118} and *yw*–exhibited vastly different fractional shortening and lifespan. Correlated with these changes was the observation that w^{1118} flies had significantly increased BM thickness compared to *yw* flies, reminiscent of aging phenotypes observed in mice [8] and disease phenotypes observed in humans [9]. Pericardin and Viking were upregulated in w^{1118} flies, leading us to hypothesize that thicker or more disorganized BM could disrupt

mechanical crosstalk or previously hypothesized tension [16] that occurs between the two muscle layers. Without such signals, outside-in signaling between muscle layers mediated by BM could be absent [46]; internal CM remodeling with age also may not occur. This could explain the decreased fractional shortening for w^{1118} flies that we have observed. Taken together, these data could present cardiac-based reasons for the severely decreased lifespan of w^{1118} flies relative to *yw;* specifically, that increased accumulation of BM proteins Pericardin, Viking, or Laminin A could be responsible for the increased BM thickness and organization leading to dysfunction in w^{1118}.

Physiological reduction in BM components correlates with increased cardiac function and improved lifespan

BM is a complex and hierarchical assembly of matrix proteins [18]. Based on our mechanical and protein expression analyses, we hypothesized that decreasing BM expression in w^{1118} may improve cardiac function. We applied cardiac restricted knockdown of *Pericardin* and *Viking*, as well as *Laminin A* due to its importance in regulating *Drosophila* heart tube morphogenesis [17,18], known upregulation in disease [9], and conserved upregulation in aged monkey and rat myocardium [10]. Reducing BM protein production decreased BM thickness in the *Drosophila* heart, but the modulation of specific matrix proteins correlated with improvement in heart tube function with age and enhanced longevity to varying degrees. For example, cardiac restricted *LanAKD* increased wall velocities at 1 week, and correlated with the greatest preservation of function with age. These data were validated using *Drosophila* lines heterozygously deficient in portions of a single chromosome spanning an ECM gene of interest. *LanA*+/– hearts experienced similar increases in diastolic dimensions as well as increased fractional shortening and heart tube wall velocities. While consistent with RNAi, these global heterozygous KO models are not as precise due to excision over a multi-gene span of the chromosome, e.g. *Vkg*+/– deficiency spans the neighboring gene *Cg25c*, which is the other collagen type IV subunit exacerbating the phenotype. Together though, these data suggest that BM proteins are more than just structural entities; rather, they are capable of regulating cardiac function with age as they change how heart tube and adjacent muscle layers interact. With considerable homology of fly BM proteins to mammals, our data suggests that targeting cardiac BM expression and resultant thickening with age or disease in mammals could improve long-term cardiac function and positively affect lifespan.

Here we have examined the effect of attenuating BM production within non-pathological levels in the *Drosophila* heart where aging occurs rapidly and interrogation of the effect of decreased ECM between muscle layers can be measured. The beneficial effects that we observed should be further examined in larger mammalian models more similar to humans where 3D microenvironments and a multitude of various fibrillar ECM and BM proteins could be explored for their effect on heart function and aging. Additionally, future work exploiting *Drosophila*'s genetic tools could allow further exploration into the cell-ECM crosstalk mediated by β1-integrin and matrix.

Materials and methods

Drosophila lines, husbandry, and culture conditions

yellow-white (*yw*) and *white-1118* (w^{1118}) served as wildtype controls. The following RNAi lines were obtained from Vienna Drosophila Center (VDRC): *UAS-Prc*^{RNAi} (#41320), *UAS-LanA*^{RNAi} (#18873), and *UAS-Vkg*^{RNAi} (#16858). The cardiac specific driver *hand-Gal4* line [47] and *Vkg-GFP* flytrap line [48] were used for RNAi silencing of genes and visualization, respectively. Briefly, UAS-transgenic males were crossed with virgin female *hand-Gal4* flies using the GAL4-UAS system as previously described [49,50]. Female progeny of *hand-Gal4* and w^{1118} served as control labeled *Hand-*w^{1118}. The following w^{1118} deficiency stocks from Bloomington were used for genetic KD validation: *Df*(*3L*)*BSC373*/*TM6C* (#24397) for deficiency of *Laminin A* referred to as *LanA*+/–, *Df* (*2L*)*BSC172*/*CyO* (#9605) for deficiency of both collagen IV alleles *Viking and Cg25c* referred to as *Vkg*+/–, and *Df*(*3L*)*BSC840*/*TM6C* (*#29024*) for deficiency of *Pericardin* referred to as *Prc*+/– [36]. w^{1118} flies served as controls for deficiency comparisons. All stocks were raised on standard agar-containing food at 25° through all life stages. Food was changed every fourth day.

Drosophila microsurgeries

Preparation of the *Drosophila* heart for ventral imaging, AFM, and tissue collection was performed as previously described [43], and did not affect heart function as previously shown [10]. Adult female flies were briefly exposed to 5 psi CO_2 (<1 min), then anesthetized with Fly Nap (Carolina Biological) for 5 min, and secured dorsal side down onto a 35 mm petri dish. The beating heart was exposed by incisions to remove head, thorax, and the ventral abdominal cuticle. Flies were then submerged in an artificial oxygenated hemolymph at 25 °C [33]. Internal organs and debris above the beating heart were all carefully aspirated away with a micropipette so as to not perturb the heart, which could result in a

hypercontractile state. The beating heart can be sustained for hours with regular oxygenation and hemolymph changes, but all experiments were performed within 1 h of microsurgery.

Immunostaining and imaging

Fluorescent labeling was performed using a modified protocol as previously described for Figs. 2, S1, S2, S3, and S4 [51]. Briefly, ventrally-exposed beating hearts were relaxed with 10 mM EGTA, then fixed with 3.7% paraformaldehyde in hemolymph, and then permeabalized in 0.1% Triton X in PBS (PBST). Samples were blocked with 1% Seablock in PBST before being incubated in primary antibody overnight at 4 °C. Samples were then washed and submersed in secondary antibodies in PBST for 60 min, washed with PBST and then PBS before mounting dorsal side down on 25 mm coverslips with Fluoromount (Southern Biotech). Fluorescence microscopy was performed on a Zeiss LSM 710 laser scanning confocal microscope at either 20 or 40× magnification. Quantification of relative fluorescent intensity for ECM proteins was performed in ImageJ via measurement of mean pixel intensity within a region of interest (ROI) selected over the heart tube (Fig. 2C) and normalized to F-actin average intensity. The following antibodies were used: mouse anti-Pericardin (1:40, EC11-s, DSHB), guinea pig anti-Laminin A (1:500) [52], rabbit anti-GFP (1:500, ab6556, Abcam), rabbit anti-Collagen IV (1:500, ab6586, Abcam), and Rhodamin Phalloidin (1:1000, Invitrogen).

Atomic force microscopy (AFM)-based nanoindentation

All indentation was performed on MFP-3D Bio Atomic Force Microscope (Asylum Research) mounted in a Ti-U fluorescent inverted scope (Nikon Instruments, Melville, NY) with 2 μm radius borosilicate glass beads mounted on a 120 pN/nm silicon nitride cantilevers (Novascan Technologies). All probes were calibrated for precise spring constant via the thermal noise method. Adult female flies with exposed beating hearts were immobilized on 25 mm glass cover slip, which is mounted on a Fluid Cell Lite coverslip holder (Asylum Research) with 1 mL of hemolymph. Hearts were checked for regular contractions and arrested with 10 mM EGTA just prior to indentation. 1 μm^2 area was probed with a 4 × 4 grid of indentations and an indentation velocity of 1 μm/s resulting in 16 force curves per replicate. All indentation curves were analyzed to by an automated software custom written in MATLAB (Mathworks) as previously described in [13,14] to calculate the elastic modulus (Pa, Pascal), or stiffness, of the myocardium. This software was further adapted to analyze the elastic modulus (Pa) of the ECM between the VM and myocardium and the thickness of this layer in μm. This analysis method can detect the presence of a third material not fit by either the ventral or cardiac fits. A third region is found if $R^2 > 0.95$ and stiffness is 25% less than the VM layer.

Proteomic analysis of *Drosophila* cardiac tissue

50 heart tubes per biological replicate were prepared and analyzed by reverse phase liquid chromatography tandem mass spectrometry (LC–MS/MS) on a Dionex Ultimate 3000 NanoLC (Thermo Scientific) connected to an Orbitrap Elite mass spectrometer (Thermo Scientific). 4 biological replicates were measured for each genotype. The analysis was operated in a data dependent acquisition (DDA) with MS1 scans acquired in the Orbitrap Elite at a resolution of 60,000, followed by tandem mass spectra acquired for the top 15 most abundant ions in the ion trap after peptide fragmentation by collision-induced dissociation. Specifically, 50 whole beating heart tubes corresponding to 80 μg of protein were cleaned, extracted and pooled into deionized water for each genotype at one week of age. Samples were washed 3 times in deionized water and then lyophilized. Lyophilized *Drosophila* hearts were solubilized in 25 μL of 9 M urea for 30 min at room temperature with agitation. Samples were diluted 1:5 (125 μL) with 50 mM Ammonium Bicarbonate, reduced with 10 mM TCEP for 30 min in the dark, and then alkylated with 15 mM Iodoacetamide for 20 min. A Trypsin/LysC solution was used to digest the samples at 60:1 ratio (protein:trypsin/lysC) overnight at 37 °C at pH 8 with constant agitation in the presence of 10% acetronitrile (ACN). After digestion, the peptide mixture was acidified with 10% Formic Acid FA to pH 2, partly dried on a speedvac to evaporate any acetonitrile, and desalted using a 30 μg microelution plate (Waters). 2 μg of peptides were resuspended in 0.1% FA and analyzed by liquid chromatography tandem mass spectrometry (LC–MS/MS) on a Dionex Ultimate 3000 NanoLC (mobile phase A: 0.1% FA in water, mobile phase B: 0.1% FA in ACN) connected to an Orbitrap Elite mass spectrometer (Thermo) equipped with a EasySpray ion source. Peptides were directly loaded onto the analytical column (PepMap RSLC C18 2 μm, 100 Å, 50 μm i.d. × 15 cm) at a flow rate of 300 nL/min using a linear gradient of 2–25% B for 120 min, 25–90% B for 5 min, then holding at 90% for 5 min and re-equilibrating at 2% B for 9 min. Temperature was set to 40 °C for both columns. The nano-source capillary temperature was set to 275 °C and the spray voltage was set to 2 kV. MS1 scans were acquired in the Orbitrap Elite at a resolution of 60,000 full-width, half max (FWHM) with a target of 1×10^6 ions over a maximum of 500 ms. MS2 spectra were acquired for the top 15 ions from each MS1 scan in

normal scan mode in the ion trap with a target setting of 1×10^4 ions, an accumulation time of 100 ms, and an isolation width of 2 Da. The normalized collision energy was set to 35% and one microscan was acquired for each spectra. All raw data from the orbitrap elite were converted to centroided mzXML format for peaklist generation using proteowizard (Version 3.0.8990). The mzXML files were then searched using the Comet search algorithm running through the Trans Proteomic Pipeline (TPP; Version 4.8.0) against Swiss-prot database of reviewed *Drosophila* protein FASTA sequences with randomized decoys appended. Carbamidomethylation of cysteine was set as a fixed modification and oxidization of methionine set as a variable modification. Tolerance for mass error was set to 20 ppm for precursors and 1 da for fragments. Trypsin was set as the digestion enzyme with up to two missed cleavages allowed. Peptide spectral match confidence was determined using the Peptide Prophet algorithm built into the xinteract tool on the TPP, using high accurate mass binning, retention time information, and non-parametric modeling settings. Peptides with >95% probability were uploaded into Skyline Software to perform MS1 extraction and quantification as previously described [26]. We required all peptides to fit a retention time alignment with an $r^2 < 0.95$ and to demonstrate an isotope dot product correlation scores >0.8. Only proteotypic peptides were used for quantitative analysis. Results of the MS1 filtering were exported for input to msstats an R-based tool for proteomic data analysis [53]. Precursor intensities were median normalized and protein level inference computed using the linear mixed model. Median normalized MS1 intensity values are provided for each peptide with its corresponding protein ID obtained from Unitprot of the 4 biological replicates of each genotype w^{1118} and *yw* in Supplemental Tables S1 and S2 respectively. STRAP analysis for ECM and cytoskeletal related proteins are provided in Supplemental Table S3 and plotted with MS1 intensity values in Fig. 3A. Differential expression of proteins is provided by distance calculations provided in Supplemental Table S3 and plotted in Fig. 2B. Additional proteomic methods and analysis related to rhesus macaque and *rattus norvegicus* mass spectrometry used to measure protein expression in Supplemental Table S4 are described elsewhere [10].

Quantitative PCR analysis

RNA was extracted from 15 whole, beating heart tubes cleaned of any excess fat or debris with a fine micropipette by Zymo Research Quick RNA Micro-Prep kit. This collection of 15 hearts constituted one biological replicate. RNA concentration and purity was verified via Nanodrop. Reverse transcription to synthesize first strand cDNA was performed on equal quantities of RNA per sample. For quantitative PCR each reaction was run with 1 μL template cDNA, 2.5 μL each forward and reverse primer, 6.5 μL DEPC water, and 12.5 μL SYBR-green intercalating dye (Applied Biosystems). Each gene was analyzed for at least 4 biological replicates per genotype and age and absolute quantity was calculated by comparison to a standard curve for data in Supplemental Fig. S3. For the transgenics they were first normalized to housekeeper *GapDH2* and then displayed as a ratio of given genotype/control quantity. The primers used were presented in 5′ to 3′: *Pericardin* Fwd (CGGAGGACAGGCTACAATAA) Rev (CCAATACCAGGCTGACCTATAA), *LamininA* Fwd (GTTCTTCTACGGCAGGGATAAG) Rev (CTCCACCTTCACCCAAACTAA), *Viking* Fwd (GATCTACGACAACACTGGTGAG) Rev (TTCGCCACGAAGTCCAATAG), *Myospheriod* (β1-integrin) Fwd (AAACACTGCGAGTGCGACAAC) Rev (ACATGTATCGTTGGACTCCTG), *GapDH2* Fwd (TTCTTCAGCGACACCCATTC) Rev (CGTTGTCGTACCACGAGATTAG).

Heartbeat analysis and viscous loading assay

Fly hearts were ventrally exposed and 20 s movies were taken at a rate of 120–150 frames per second (FPS) using a Hamamatsu EM-CCD digital camera mounted on a Leica DM LFSA microscope with a 10X water-immersion lens and HCI imaging software in regular hemolymph. Viscous loading assay was then performed as previously described [10,12]. Briefly, the hearts after being imaged in regular hemolymph were then washed with 10% w/v Ficoll (relative viscosity 5) in oxygenated hemolymph, allowed to equilibrate for 20 min, and then imaged again. Hearts were then washed with 20% w/v Ficoll (relative viscosity 20), equilibrated for 20 min, and imaged again. Over 20 biological replicates were imaged per genotype and age. Images were analyzed and motion-mode kymographs, or m-modes, were generated using the Semi-automated Optical Heart Beat Analysis software as previously published [12,54], and calculation of systolic and diastolic lengths, fractional shortening, and shortening (contraction) and lengthening (relaxation) velocities were obtained by the modified software allowing for phase analysis [12]. Shortening and lengthening velocities were calculated by dividing the contraction length by either the contraction and lengthening intervals, i.e. the time between the start of contraction and the start of isovolumic systole and the time between the end of isovolumic systole and start of isovolumic diastole, respectively. Based on the Hill's equation [55] a least square's fit was performed on the average shortening velocities for each genotype as a function of relative viscosity using a MATLAB script as previously published and plotted in Fig. 5 [10].

Fits are displayed over the relative viscosity ranges tested. Coefficients are provided in Supplemental Table S8. A least squares fit was also performed for the average lengthening velocities and are displayed over relative viscosity ranges tested.

Longevity assay

For survival experiments in Figs. 1 and 5, virgin females were collected for 10 days after which they were briefly anesthetized by CO_2 and separated into groups of 25 flies in each vial. The flies were kept at 25°. Dead flies were counted every 2 days after transfer onto new standard agar-containing food. Each experiment consisted of 200–250 flies. Data were analyzed using Prism 5.0a (Graphpad Software, Inc.). Further details are provided in Supplemental Table S9.

Statistical methods

All data were checked for Gaussian distribution prior to analysis using D'agnostino-Pearson omnibus normality test. Non-parametric Student's two-tailed t-test with unequal variances assumption was used for analyzing AFM measurements when comparing more than one genotype at a specific age. Two-way analysis of variance (ANOVA) was used when comparing 2 or more groups at more than one condition such as relative viscosity in the ficoll assay followed by a Bonferroni multiple comparisons post hoc test of significances. Significances are displayed on the graph indicating load/genotype as source of variance with Bonferroni post hoc test results denoted over specific point comparisons. Deficiency line data for physiological analyses of high-speed movies were analyzed via one-way-anova with post hoc dunnetts's multiple comparisons test. Lifespan analyses were performed using a log-rank analysis (Mantel-Cox test). In all cases $p < 0.05$ were taken as significant. All statistical analyses were performed using Prism 5.0a (Graphpad Software, Inc) except for the use of MSstats: an R package for statistical analysis for quantitative mass spectrometry–based proteomic experiments [53]. Specific analyses used are indicated in figure legends. All in situ experiments were performed with biological replicates of 15–30 flies unless otherwise indicated while genetic or protein expression experiments represent <4 biological replicates of 15–50 pooled fly hearts as indicated in the legends.

Supplementary data to this article can be found online at doi:10.1016/j.matbio.2016.10.008.

Competing interests

The authors declare no competing financial interests.

Author contributions

Conceptualization: A.O.S., G.K., and A.J.E.; Methodology: A.O.S., G.K., R.B., and J.E.V.E.; Investigation: A.O.S., G.K., S.P., and K.R.; Writing: A.O.S and A.J.E.; Review and Editing: A.O.S., G.K., R.B., J.E.V.E., and A.J.E.; Funding Acquisition: A.O.S., G.K., and A.J.E.; Supervision: J.E.V.E. and A.J.E.

Acknowledgements

yellow-white (*yw*), *white-1118* (w^{1118}), *Viking-GFP* flytrap, and Hand-*Gal4* fly lines were generous gifts from Georg Vogler (Sanford Burnham Medical Research Institute, La Jolla, CA). All other stocks were obtained from the Bloomington Drosophila Stock Center (NIH P40OD018537). The authors would like to thank Dr. Karen Ocorr and Georg Vogler for technical assistant in data acquisition and analysis and Dr. Anthony Cammarato for helpful comments. This work was directly supported by grants from the National Institutes of Health (T32HL105373, R01AG045428, DP2OD006460, R21HL106529, and 1F31HL131137), and the American Heart Association (13PRE14410037 and 15PRE25090334).

Received 23 September 2016;
Received in revised form 19 October 2016;
Accepted 22 October 2016
Available online 25 October 2016

Keywords:
Drosophila;
Laminin A;
Basement membrane;
Extracellular matrix;
Aging

Non-standard abbreviations and acronyms used:
Extracellular Matrix, ECM; Cardiomyocytes, CM; Ventral Muscle, VM; Basement Membrane, BM; Intercalated Disc, ID; Atomic Force Microscopy, AFM; Frames Per Second, FPS; Liquid Chromatography-Tandem Mass Spectrometry, LC–MS/MS; Data Dependent Acquisition, DDA; Knockdown, KD; Software Tool for Rapid Annotation of Proteins, STRAP; Vienna Drosophila Center, VDRC; Basic Local Alignment Search Tool, BLAST.

References

[1] B.A. Borlaug, M.M. Redfield, Diastolic and systolic heart failure are distinct phenotypes within the heart failure spectrum, Circulation 123 (18) (2011) 2006–2013 (discussion 2014).

[2] H. Iwano, W.C. Little, Heart failure: what does ejection fraction have to do with it? J. Cardiol. 62 (1) (2013) 1–3.
[3] E.G. Lakatta, Age-associated cardiovascular changes in health: impact on cardiovascular disease in older persons, Heart Fail. Rev. 7 (1) (2002) 29–49.
[4] S.C. Lieber, N. Aubry, J. Pain, G. Diaz, S.J. Kim, S.F. Vatner, Aging increases stiffness of cardiac myocytes measured by atomic force microscopy nanoindentation, Am. J. Physiol. Heart Circ. Physiol. 287 (2) (2004) H645–H651.
[5] S. Hein, W.H. Gaasch, J. Schaper, Giant molecule titin and myocardial stiffness, Circulation 106 (11) (2002) 1302–1304.
[6] J. Favor, C.J. Gloeckner, D. Janik, M. Klempt, A. Neuhäuser-Klaus, W. Pretsch, W. Schmahl, L. Quintanilla-Fend, Type IV procollagen missense mutations associated with defects of the eye, vascular stability, the brain, kidney function and embryonic or postnatal viability in the mouse, *Mus musculus*: an extension of the Col4a1 allelic series and the identification of the first two Col4a2 mutant alleles, Genetics 175 (2) (2007) 725–736.
[7] T. Van Agtmael, L. Bruckner-Tuderman, Basement membranes and human disease, Cell Tissue Res. 339 (1) (2010) 167–188.
[8] L.E. de Castro Brás, H. Toba, C.F. Baicu, M.R. Zile, S.T. Weintraub, M.L. Lindsey, A.D. Bradshaw, Age and SPARC change the extracellular matrix composition of the left ventricle, Biomed. Res. Int. 2014 (2014) 810562.
[9] E.H. Kim, V.I. Galchev, J.Y. Kim, S.A. Misek, T.K. Stevenson, M.D. Campbell, F.D. Pagani, S.M. Day, T.C. Johnson, J.G. Washburn, K.L. Vikstrom, D.E. Michele, D.E. Misek, M.V. Westfall, Differential protein expression and basal lamina remodeling in human heart failure, Proteomics Clin. Appl. 10 (5) (2016) 585–596.
[10] G. Kaushik, A. Spenlehauer, A.O. Sessions, A.S. Trujillo, A. Fuhrmann, Z. Fu, V. Venkatraman, D. Pohl, J. Tuler, M. Wang, E.G. Lakatta, K. Ocorr, R. Bodmer, S.I. Bernstein, J.E. Van Eyk, A. Cammarato, A.J. Engler, Vinculin network-mediated cytoskeletal remodeling regulates contractile function in the aging heart, Sci. Transl. Med. 7 (292) (2015) (292ra99).
[11] A. Cammarato, C.H. Ahrens, N.N. Alayari, E. Qeli, J. Rucker, M.C. Reedy, C.M. Zmasek, M. Gucek, R.N. Cole, J.E. Van Eyk, R. Bodmer, B. O'Rourke, S.I. Bernstein, D.B. Foster, A mighty small heart: the cardiac proteome of adult *Drosophila melanogaster*, PLoS One 6 (4) (2011), e18497.
[12] A. Cammarato, S. Ocorr, K. Ocorr, Enhanced assessment of contractile dynamics in drosophila hearts, Biotechniques 58 (2) (2015) 77–80.
[13] G. Kaushik, A. Fuhrmann, A. Cammarato, A.J. Engler, In situ mechanical analysis of myofibrillar perturbation and aging on soft, bilayered Drosophila myocardium, Biophys. J. 101 (11) (2011) 2629–2637.
[14] G. Kaushik, A.C. Zambon, A. Fuhrmann, S.I. Bernstein, R. Bodmer, A.J. Engler, A. Cammarato, Measuring passive myocardial stiffness in *Drosophila melanogaster* to investigate diastolic dysfunction, J. Cell. Mol. Med. 16 (8) (2012) 1656–1662.
[15] L.T. Wasserthal, Drosophila flies combine periodic heartbeat reversal with a circulation in the anterior body mediated by a newly discovered anterior pair of ostial valves and 'venous' channels, J. Exp. Biol. 210 (Pt 21) (2007) 3707–3719.
[16] C. Lehmacher, B. Abeln, A. Paululat, The ultrastructure of Drosophila heart cells, Arthropod. Struct. Dev. 41 (5) (2012) 459–474.
[17] T.A. Haag, N.P. Haag, A.C. Lekven, V. Hartenstein, The role of cell adhesion molecules in Drosophila heart morphogenesis: faint sausage, shotgun/DE-cadherin, and laminin A are required for discrete stages in heart development, Dev. Biol. 208 (1) (1999) 56–69.
[18] J.M. Urbano, C.N. Torgler, C. Molnar, U. Tepass, A. López-Varea, N.H. Brown, J.F. de Celis, M.D. Martín-Bermudo, Drosophila laminins act as key regulators of basement membrane assembly and morphogenesis, Development 136 (24) (2009) 4165–4176.
[19] D. Hollfelder, M. Frasch, I. Reim, Distinct functions of the laminin beta LN domain and collagen IV during cardiac extracellular matrix formation and stabilization of alary muscle attachments revealed by EMS mutagenesis in Drosophila, BMC Dev. Biol. 14 (2014) 26.
[20] J.C. Pastor-Pareja, T. Xu, Shaping cells and organs in Drosophila by opposing roles of fat body-secreted Collagen IV and perlecan, Dev. Cell 21 (2) (2011) 245–256.
[21] T. Volk, S. Wang, B. Rotstein, A. Paululat, Matricellular proteins in development: perspectives from the Drosophila heart, Matrix Biol. 37 (2014) 162–166.
[22] A. Chartier, S. Zaffran, M. Astier, M. Semeriva, D. Gratecos, Pericardin, a Drosophila type IV collagen-like protein is involved in the morphogenesis and maintenance of the heart epithelium during dorsal ectoderm closure, Development 129 (13) (2002) 3241–3253.
[23] M. Drechsler, A.C. Schmidt, H. Meyer, A. Paululat, The conserved ADAMTS-like protein lonely heart mediates matrix formation and cardiac tissue integrity, PLoS Genet. 9 (7) (2013), e1003616.
[24] J. Vanderploeg, L.L. Vazquez Paz, A. MacMullin, J.R. Jacobs, Integrins are required for cardioblast polarisation in Drosophila, BMC Dev. Biol. 12 (2012) 8.
[25] J.L. Spencer, V.N. Bhatia, S.A. Whelan, C.E. Costello, M.E. McComb, STRAP PTM: software tool for rapid annotation and differential comparison of protein post-translational modifications, Curr. Protoc. Bioinformatics 13 (1322) (2013) 13.22.1–13.22.36.
[26] B. Schilling, M.J. Rardin, B.X. MacLean, A.M. Zawadzka, B.E. Frewen, M.P. Cusack, D.J. Sorensen, M.S. Bereman, E. Jing, C.C. Wu, E. Verdin, C.R. Kahn, M.J. Maccoss, B.W. Gibson, Platform-independent and label-free quantitation of proteomic data using MS1 extracted ion chromatograms in skyline: application to protein acetylation and phosphorylation, Mol. Cell. Proteomics 11 (5) (2012) 202–214.
[27] S.F. Altschul, T.L. Madden, A.A. Schäffer, J. Zhang, Z. Zhang, W. Miller, D.J. Lipman, Gapped BLAST and PSI-BLAST: a new generation of protein database search programs, Nucleic Acids Res. 25 (17) (1997) 3389–3402.
[28] M. Aumailley, N. Smyth, The role of laminins in basement membrane function, J. Anat. 193 (Pt 1) (1998) 1–21.
[29] J.B. Duffy, GAL4 system in Drosophila: a fly geneticist's Swiss army knife, Genesis 34 (1–2) (2002) 1–15.
[30] G. Dietzl, D. Chen, F. Schnorrer, K.C. Su, Y. Barinova, M. Fellner, B. Gasser, K. Kinsey, S. Oppel, S. Scheiblauer, A. Couto, V. Marra, K. Keleman, B.J. Dickson, A genome-wide transgenic RNAi library for conditional gene inactivation in Drosophila, Nature 448 (7150) (2007) 151–156.
[31] M.C. Viswanathan, G. Kaushik, A.J. Engler, W. Lehman, A. Cammarato, A *Drosophila melanogaster* model of diastolic dysfunction and cardiomyopathy based on impaired troponin-T function, Circ. Res. 114 (2) (2014) e6–17.
[32] O. Taghli-Lamallem, T. Akasaka, G. Hogg, U. Nudel, D. Yaffe, J.S. Chamberlain, K. Ocorr, R. Bodmer, Dystrophin deficiency in Drosophila reduces lifespan and causes a dilated cardiomyopathy phenotype, Aging Cell 7 (2) (2008) 237–249.

[33] K. Ocorr, N.L. Reeves, R.J. Wessells, M. Fink, H.S. Chen, T. Akasaka, S. Yasuda, J.M. Metzger, W. Giles, J.W. Posakony, R. Bodmer, KCNQ potassium channel mutations cause cardiac arrhythmias in Drosophila that mimic the effects of aging, Proc. Natl. Acad. Sci. U. S. A. 104 (10) (2007) 3943–3948.
[34] M. Nishimura, C. Kumsta, G. Kaushik, S.B. Diop, Y. Ding, J. Bisharat-Kernizan, H. Catan, A. Cammarato, R.S. Ross, A.J. Engler, R. Bodmer, M. Hansen, K. Ocorr, A dual role for integrin-linked kinase and beta1-integrin in modulating cardiac aging, Aging Cell 13 (3) (2014) 431–440.
[35] A. Cammarato, C.M. Dambacher, A.F. Knowles, W.A. Kronert, R. Bodmer, K. Ocorr, S.I. Bernstein, Myosin transducer mutations differentially affect motor function, myofibril structure, and the performance of skeletal and cardiac muscles, Mol. Biol. Cell 19 (2) (2008) 553–562.
[36] A.L. Parks, K.R. Cook, M. Belvin, N.A. Dompe, R. Fawcett, K. Huppert, L.R. Tan, C.G. Winter, K.P. Bogart, J.E. Deal, M.E. Deal-Herr, D. Grant, M. Marcinko, W.Y. Miyazaki, S. Robertson, K.J. Shaw, M. Tabios, V. Vysotskaia, L. Zhao, R.S. Andrade, K.A. Edgar, E. Howie, K. Killpack, B. Milash, A. Norton, D. Thao, K. Whittaker, M.A. Winner, L. Friedman, J. Margolis, M.A. Singer, C. Kopczynski, D. Curtis, T.C. Kaufman, G.D. Plowman, G. Duyk, H.L. Francis-Lang, Systematic generation of high-resolution deletion coverage of the *Drosophila melanogaster* genome, Nat. Genet. 36 (3) (2004) 288–292.
[37] J. Shahab, C. Baratta, B. Scuric, D. Godt, K.J. Venken, M.J. Ringuette, Loss of SPARC dysregulates basal lamina assembly to disrupt larval fat body homeostasis in *Drosophila melanogaster*, Dev. Dyn. 244 (4) (2015) 540–552.
[38] G. Wolfstetter, A. Holz, The role of LamininB2 (LanB2) during mesoderm differentiation in Drosophila, Cell. Mol. Life Sci. 69 (2) (2012) 267–282.
[39] M. Ziehm, M.D. Piper, J.M. Thornton, Analysing variation in Drosophila aging across independent experimental studies: a meta-analysis of survival data, Aging Cell 12 (5) (2013) 917–922.
[40] A. Heling, R. Zimmermann, S. Kostin, Y. Maeno, S. Hein, B. Devaux, E. Bauer, W.P. Klövekorn, M. Schlepper, W. Schaper, J. Schaper, Increased expression of cytoskeletal, linkage, and extracellular proteins in failing human myocardium, Circ. Res. 86 (8) (2000) 846–853.
[41] E. Dworatzek, I. Baczko, G. Kararigas, Effects of aging on cardiac extracellular matrix in men and women, Proteomics Clin. Appl. (2015).
[42] M. Nishimura, K. Ocorr, R. Bodmer, J. Cartry, Drosophila as a model to study cardiac aging, Exp. Gerontol. 46 (5) (2011) 326–330.
[43] G. Vogler, K. Ocorr, Visualizing the beating heart in Drosophila, J. Vis. Exp. 31 (2009).
[44] T.K. Borg, K. Rubin, E. Lundgren, K. Borg, B. Obrink, Recognition of extracellular matrix components by neonatal and adult cardiac myocytes, Dev. Biol. 104 (1) (1984) 86–96.
[45] M.L. McCain, H. Lee, Y. Aratyn-Schaus, A.G. Kléber, K.K. Parker, Cooperative coupling of cell-matrix and cell–cell adhesions in cardiac muscle, Proc. Natl. Acad. Sci. U. S. A. 109 (25) (2012) 9881–9886.
[46] A.M. Samarel, Costameres, focal adhesions, and cardiomyocyte mechanotransduction, Am. J. Physiol. Heart Circ. Physiol. 289 (6) (2005) H2291–H2301.
[47] Z. Han, E.N. Olson, Hand is a direct target of Tinman and GATA factors during Drosophila cardiogenesis and hematopoiesis, Development 132 (15) (2005) 3525–3536.
[48] X. Morin, R. Daneman, M. Zavortink, W. Chia, A protein trap strategy to detect GFP-tagged proteins expressed from their endogenous loci in Drosophila, Proc. Natl. Acad. Sci. U. S. A. 98 (26) (2001) 15050–15055.
[49] N. Staudt, A. Molitor, K. Somogyi, J. Mata, S. Curado, K. Eulenberg, M. Meise, T. Siegmund, T. Häder, A. Hilfiker, G. Brönner, A. Ephrussi, P. Rørth, S.M. Cohen, S. Fellert, H.R. Chung, O. Piepenburg, U. Schäfer, H. Jäckle, G. Vorbrüggen, Gain-of-function screen for genes that affect Drosophila muscle pattern formation, PLoS Genet. 1 (4) (2005), e55.
[50] Y. Bidet, T. Jagla, J.P. Da Ponte, B. Dastugue, K. Jagla, Modifiers of muscle and heart cell fate specification identified by gain-of-function screen in Drosophila, Mech. Dev. 120 (9) (2003) 991–1007.
[51] N.N. Alayari, G. Vogler, O. Taghli-Lamallem, K. Ocorr, R. Bodmer, A. Cammarato, Fluorescent labeling of Drosophila heart structures, J. Vis. Exp. 32 (2009).
[52] N. Harpaz, T. Volk, A novel method for obtaining semi-thin cross sections of the Drosophila heart and their labeling with multiple antibodies, Methods 56 (1) (2012) 63–68.
[53] M. Choi, C.Y. Chang, T. Clough, D. Broudy, T. Killeen, B. MacLean, O. Vitek, MSstats: an R package for statistical analysis of quantitative mass spectrometry-based proteomic experiments, Bioinformatics 30 (17) (2014) 2524–2526.
[54] M. Fink, C. Callol-Massot, A. Chu, P. Ruiz-Lozano, J.C. Izpisua Belmonte, W. Giles, R. Bodmer, K. Ocorr, A new method for detection and quantification of heartbeat parameters in Drosophila, zebrafish, and embryonic mouse hearts, Biotechniques 46 (2) (2009) 101–113.
[55] C.Y. Seow, Hill's equation of muscle performance and its hidden insight on molecular mechanisms, J. Gen. Physiol. 142 (6) (2013) 561–573.